ANALYSIS OF VEHICLE ROOF WEAKNESS AND POTENTIAL FOR NECK INJURIES FROM EXPERIMENTAL AND SIMULATED DYNAMIC ROLLOVER TESTS

Mario Mongiardini
Raphael H. Grzebieta
Garrett A. Mattos
Mike Bambach
George Rechnitzer
Transport and Road Safety (TARS) - University of New South Wales,
Australia

Andrew S. McIntosh
McIntosh Consultancy & Research Pty Ltd,
Australia

Ross Dal Nevo
Roads and Maritime Services (RMS), Crashlab, New South Wales
Australia

Paper Number 15-0131

ABSTRACT

Despite the considerable rollover crashworthiness research carried out to date, there is still a need to establish exactly how spine and neck injuries occur to a seat-belted occupant during a rollover. This paper details an experimental and Finite Element (FE) analysis aimed at demonstrating how a stronger vehicle roof can reduce the potential for neck injuries to a seat belted occupant seated in the front on the rollover far-side.

An analysis was carried out of the head-torso kinematics of a seat-belted Anthropomorphic Test Device (ATD) measured during two rollover crash tests conducted on a weak- and strong-roof sport utility vehicle (SUV), respectively. Both experimental laboratory rollover tests were performed under the same nominal conditions using the original Center for Injury Research (CFIR) Jordan Rollover System (JRS) located in Goleta, California. Further, a comparison of the ATD kinematics was then carried out using data obtained from detailed FE simulations of vehicle rollovers carried out using the FE model of the University of New South Wales (UNSW) JRS located in Sydney Australia, and an FE model of a SUV, first with the original production roof and then with a reinforced roof.

The analysis of the experimental tests indicated that an excessive roof crush would likely cause the head to be captured within the crush zone long enough for the torso to apply a large inertial axial-compression load to the neck. In contrast, a stronger roof continuously guides the occupant's head moving it along an arc in a smoother manner, thus reducing any significant change in velocity between the head and torso, and any consequent inertial axial-compression loading. However, preliminary computer simulations confirm this mechanism only in part, and further simulations of the refined computer model of the UNSW JRS and SUV models are being conducted and will be reported on when completed.

INTRODUCTION

Although vehicle rollovers are relatively rare events, they are particularly dangerous crash modes with one of the highest fatality rates per crash. Generally, rollovers are responsible for 20 to 35 percent of the total fatalities in vehicle crashes, with specific percentages varying from country to country. Specifically, in the USA, vehicle rollover crashes account for around 35 percent of the total motor-vehicle road crash fatalities [1]. Similarly, in Australia, coronial investigations indicated that 27 percent of the occupants killed in a vehicle crash are involved in vehicle rollovers. Studies of rollover-related deaths in Australia found that around half of the victims were not wearing a seat belt [2,3], with the majority being ejected from the vehicle. Nonetheless, the remaining half of rollover-related fatalities involved properly restrained occupants, clearly indicating the magnitude of the risk for serious injuries and fatalities during vehicle rollover crashes, even for restrained occupants.

Understanding the mechanisms that cause severe injuries during vehicle rollovers is essential to develop future effective countermeasures, such as restraints and curtain airbags. In rollover crashes, spine and neck injuries account for around one-third of the total serious or fatal injuries [4,5]. There are a range of mechanisms proposed among researchers in regards to how an occupant's neck and spine are being injured in rollover crashes. Initially, Moffat [6] and others [7-9] proposed that such injuries result from a diving-type mechanism and that, consequently, roof strength is not causal to the degree of injury. He claimed that it did not matter that the roof crushed around the head, neck and torso of the occupant once that part of roof where the head was located inside the vehicle came into contact with the ground [10]. According to the diving theory, occupant injuries occurring in rollover crashes are simply associated with the severity of the rollover. In contrast, work by Brumbelow [11,12] and others [13-17] using real-world statistical crash data reveal some form of a relationship existing between serious and fatal injuries and roof crush and/or roof strength. Moreover, some of the authors have previously shown mathematically that when roof

crush occurs, neck loading is exacerbated [10,18,19]. More interesting is that Rechnitzer and Lane [18] indicated more than 20 years ago that entrapment of the occupant's head by the side header rail could lead to spinal cord injuries even under low levels of roof intrusion. However, when there is considerable roof crush the neck loading is exacerbated and significantly higher in these circumstances than in the case of low intrusion as discussed below.

However, the arguments presented by researchers advocating a causal relationship between roof crush and neck injuries are still being debated. In particular, the diving and the roof crush mechanisms have been found difficult to separate because neck loading resulting from either mechanism cannot be distinguished mathematically from each other [10]. Either mechanism appears to occur when observing the vehicle and occupant relative to the roadway inertial frame. Camera views taken inside the vehicle (i.e., relative to the vehicle reference system) highlight neck compression resulting from roof crush but, when viewed outside the vehicle (i.e., the roadway inertial reference system), the Anthropomorphic Test Device (ATD) appears to be diving into the roadway when the vehicle's far-side roof crushes against it. However, the difference is subtle albeit noticeable as pointed out in [20] and in Figure 1. Nonetheless, injuries occur in conjunction with considerable roof crush.

Despite extensive rollover crashworthiness research having been carried out so far, there is still a need to establish exactly how spine and neck injuries occur to a seat-belted occupant during a rollover. This paper aims at demonstrating how a stronger vehicle roof can reduce the potential for neck injuries to a properly restrained occupant seated in the front seat on the rollover far-side (i.e., the side opposite to the leading side of the rollover). The authors propose as a potential injury mechanism that, when considerable roof crush occurs, the head movement relative to the vehicle's center of mass (CoG) is associated with an amplification of the neck loading (Figure 2). This is due to an increase in inertial compressive load being applied by the torso to the neck as it keeps moving towards the head [20]. In contrast, when a strong roof limits the extent of the roof crush, the ATD's head position relative to the vehicle's CoG does not change to the same extent as in the case of the weak roof vehicle. The head is effectively guided away by the strong roof and allowed to continue smoothly in its motion path relative to roadway. Whilst some torso augmentation occurs to the neck, the neck load induced is smaller than that when the roof is weak (Figure 3).

An analysis was carried out of the head-torso kinematics of a seat-belted ATD measured during two rollover crash tests conducted on a weak- and strong-roof vehicle, respectively. Both rollover tests were performed under the same nominal conditions using the CFIR JRS [21]. Further, a comparison of the ATD kinematics was then carried out using data obtained from detailed FE simulations of vehicle rollovers carried out using the FE model of the UNSW JRS (located in Sydney Australia) and an FE model of a SUV, first with the original production roof and then with a reinforced roof.

The analysis of the experimental tests indicated that excessive roof crush in the right circumstances can cause the head to be captured within the crush zone long enough for the torso to apply a large inertial axial load onto the neck. However, the author's preliminary computer simulations have yet to fully demonstrate this mechanism using FE modelling. Nevertheless, some interesting results were generated and are discussed. Further analysis with both experimental tests and refined computer models of the UNSW JRS and SUV models are being conducted and will be reported on when completed.

EXPERIMENTAL ANALYSIS

An analysis was carried out of the ATD kinematics and dynamics during two rollover crash tests conducted using the CFIR JRS [22,23]. Each test was performed on a different SUV: a Jeep Grand Cheeroke with a roof Strength to Weight Ratio (SWR) of 2.2; and a Volvo XC90 with an SWR of 4.6. The SWR is the peak load measured within 127 mm (5 in) of platen displacement divided by the kerb weight of the vehicle during a one-sided quasi-static roof crush test. The crush test is carried out using a rigid flat platen 762 mm (30 in) wide and 1829 mm (72 in) long applied to the vehicle front A-pillar at a pitch angle of 5º and roll angle of 25º.

Measurement of the ATD's Head Motion

For both the cases of a strong- and weak-roof vehicle, frames from the high-speed videos were used to measure the movement of the ATD's head and the vehicle's Center of Gravity (CoG) relative to the roadway inertial reference system. The angle swept-arc relative to the vehicle's CoG and the front header rail were considered, as shown in the lines drawn in Figure 1. For both tests, the angular displacements, i.e., the change of the angular position between two consecutive lines drawn on the considered frames, were computed and presented as shown in Figure 2. Similarly, the distance between the ATD's head and CoG of the vehicle were also measured and compared and shown in Figure 2.

Kinematics of ATD's Head with Strong and Weak Roof

Interestingly, in the test with the strong-roof vehicle, the ATD's head continued to move through an arc, albeit the velocity of the ATD's head slows down more rapidly for the stronger roof vehicle compared to the weak roof vehicle. In the weak roof vehicle, the distance between vehicle's CoG relative to the ATD's head increases to a lesser extent than in the case of a strong roof vehicle (Figure 2). Moreover, in the case of the weak-roof vehicle, the

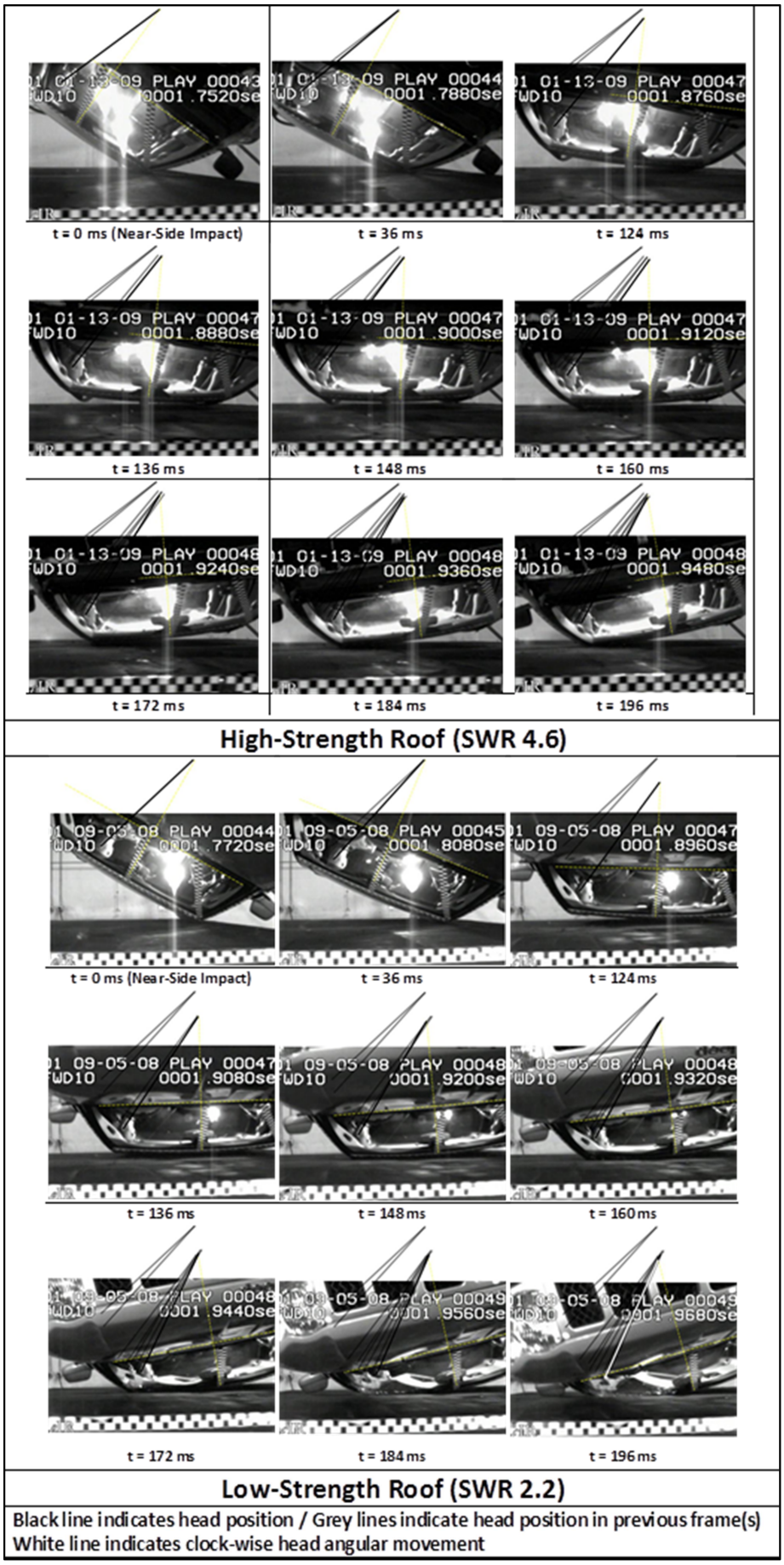

Figure 1. Movement of ATD's head relative to the vehicle's CG and the roadway – high- and low-strength roof.

ATD's head was entrapped in the roof, which subsequently buckled, pushing the head back up relative to the vehicle's CoG and the roadway, as indicated in Figure 2. The ATD torso continued to move towards the relatively entrapped (reverse thrusting) head, thus resulting in a greater axial compressive load being applied on the ATD's neck in the case of the weak roof compared to the strong roof vehicle.

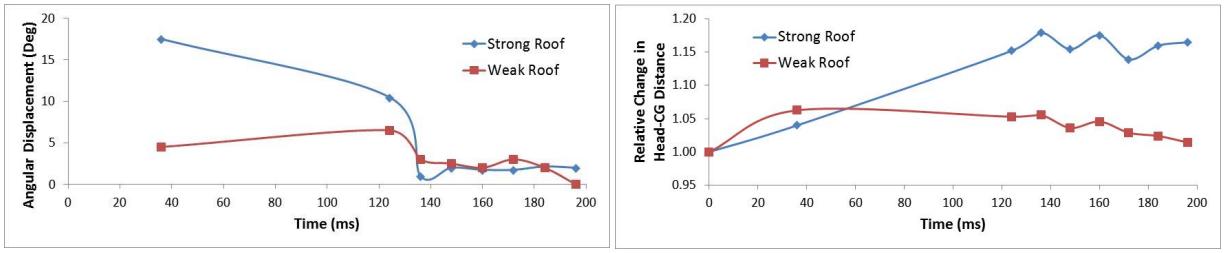

Figure 2. Left: Angular displacement of the ATD from CFIR JRS rollover crash tests of a strong roof SUV and weak roof SUV, Right: Relative change of distance from ATD head position to vehicle CoG.

ATD's Neck Load with Strong and Weak Roof

The plot of the compressive load measured by the ATD's upper-neck load cell during the two tests, an SUV with a strong-roof and an SUV with a weak-roof vehicle, are shown in Figure 3. A much higher peak compressive load of around 10 kN was measured in the test in the case of the weak-roof vehicle, compared to a peak load of about 3 kN in the case of a strong-roof vehicle.

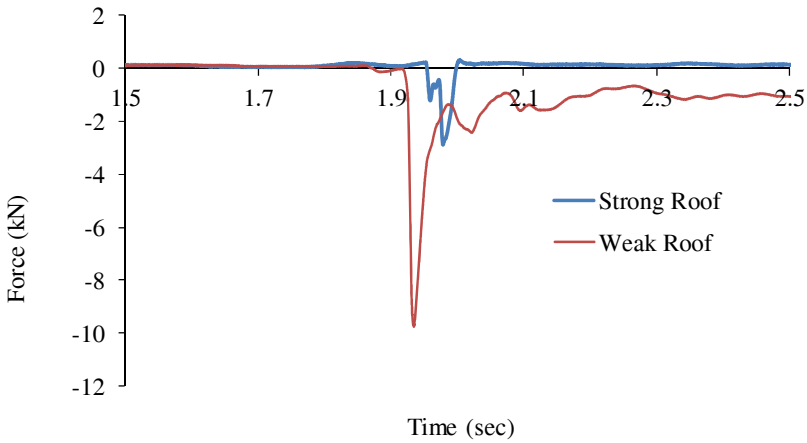

Figure 3. ATD's upper neck load from CFIR JRS rollover crash tests of a strong roof SUV and weak roof SUV [22,23].

COMPUTER SIMULATIONS

Computer simulations of a vehicle rollover crash were also conducted in order to confirm the observations presented above regarding the two experimental rollover crash tests of the strong roof SUV and weak roof SUV. Simulations were performed using the non-linear FE solver LS-DYNA [24].

FE Model

A detailed FE model was constructed of the UNSW JRS, which was previously developed by some of the authors [25,26]. The UNSW JRS operates under the same functional principles of the original CFIR JRS [27]. Results obtained from simulations with the UNSW JRS model were expected to be consistent with the experimental results of the two tests conducted with the CFIR JRS that were used to identify the injury mechanism. A FE model was not available for either of the two different vehicles that were used in the experimental tests (i.e., a Volvo XC90 and a Jeep Cherokee). Nevertheless, assuming that the injury mechanism is independent of any specific vehicle model and it depends on the magnitude of roof crush, it was assumed the FE model of a 2003 Ford Explorer should be capable of simulating such a neck axial loading mechanism. The Ford Explorer is a SUV, which is in the same vehicle category as the two vehicles used in the experimental tests conducted using the CFIR JRS. The FE model of the Ford Explorer was obtained from the National Analysis Crash Center (NCAC) [28] on-line calibrated models freely available and further modified to more closely simulate the actual vehicle deformation. The modifications consisted of changes to both the material and element properties of the windshield and some of the roof components. The FE model of the UNSW JRS coupled with the modified FE model of the Ford Explorer was previously validated against an experimental rollover crash test conducted using the UNSW JRS [26]. A FE model of the Hybrid III ATD, which was obtained from Livermore Software Technology Corporation (LSTC) [29], was seated in the driver position (right-hand drive configuration) and restrained using a generic three-point seatbelt model. The seatbelt model used a

combination of both shell elements and discrete elements and included slipring and retractor modelling features available in LS-DYNA.

To limit the time necessary to simulate the rollover test, as well as to minimise the potential for numerical instabilities associated with excessively long simulation periods, the FE analysis was carried out in two phases, i.e. Phase I – ATD, seatbelt and vehicle positioning simulation, and Phase II – reduced model impact simulation. In Phase I the whole vehicle in the UNSW JRS is gradually accelerated to the desired roll rate, then it is released at the appropriate roll angle and allowed to free drop under gravity similar to how it occurs in the actual experimental crash test. This ensures that the ATD position, seatbelt configuration and vehicle response during a rollover just prior to the roof impacting the roadbed is simulated accurately. Thus the ATD position, seatbelt configuration and vehicle conditions just prior to the roof impacting roadbed are noted and stored. For Phase II the model was reduced as shown in Figure 4 and Figure 5, and the initial conditions retrieved from Phase I were assigned to the reduced Phase II FE model, i.e. set to the same conditions as those that were measured at the time the vehicle's roof started impacting the roadbed.

Modelling Issues and Validation

Determining the proper ATD initial conditions during Phase I as well as implementing these conditions at the beginning of Phase II proved to be more challenging than what was initially thought. In the Phase I simulation, the sash part of the three-point FE seatbelt had not slipped off the FE ATD's right shoulder in contrast to what occurred in the actual experimental CFIR JRS test where the sash had slipped off the ATD's shoulder. Also, the Phase I simulation did not completely replicate the change in direction of the ATD's movement that was observed in the experimental test just before the vehicle impacted the roadbed. An analysis of the test high-speed videos showed that the initial ATD movement towards the vehicle's center console gradually slowed down and the ATD eventually started to swing back towards the far-side door. In contrast, in the Phase I simulation, the FE ATD kept moving in the direction of the center console until the FE vehicle's roof impacted the roadbed. Both these differences in the FE seatbelt and FE ATD's movement appear to have affected establishing the initial position of the FE ATD and FE seat belt model for the Phase II simulation. This resulted in some differences in the simulated FE ATD response during the impact compared with the experimental test results. Further, a limitation in LS-DYNA prevented imposing independently an initial velocity field to the ATD and the vehicle model at the start of the Phase II impact simulation, making the simulation task challenging.

A partial validation of the FE model of the UNSW JRS and the FE vehicle coupled with the FE ATD was accomplished. However further work is required. The FE model (UNSW JRS, vehicle, ATD and seat belt) validation was based on the ATD kinematics that was measured during an experimental test of the UNSW JRS combined with the Explorer [25,26,27]. A comparison of the simulated FE ATD kinematics and the kinematics observed during the experimental test is shown in the sequential frames in Figure 4. The simulated ATD kinematics were different from what was observed during the actual rollover crash test, which was likely due to the above mentioned issues related to the ATD and seatbelt initial configurations at impact.

There was a further complicating modelling issue. In the experimental test, at the start of the vehicle's roof impact with the roadbed, the ATD was offset from the seat cushion due to the vehicle roll position. During the first 150 ms after the initial vehicle impact, the ATD's posterior offset from the seat cushion remained constant. Unfortunately, in the simulation, the FE ATD kept moving away from the FE seat cushion, towards the FE vehicle roof. This incompatibility between the test and FE simulation resulted in two subsequent major differences when comparing the results of the FE simulation to the experimental test in terms of (i) location where the head impacted the roof and (ii) magnitude of bending of the ATD's neck. Further, in the experimental test, the ATD's head impacted the side of the roof in proximity to the far-side rail. In contrast, in the simulation the initial impact of the FE ATD's head against the roof occurred at a location directly above the center of the driver's seat, i.e. further inboard of the side header rail. Also, more extensive bending of the FE ATD's neck occurred in the simulation, likely due to the FE ATD's posterior continually moving away from the seat cushion towards the roof.

Analysis of Simulations with Weak and Strong Roof

The FE model was then used to simulate a rollover under the same initial conditions as in the baseline experimental test, but using a modified version of the Explorer model with a stronger roof. To increase the roof strength, the yield stress and the wall thickness of the A- and B-pillars and the roof header were increased by 50 percent and one millimeter, respectively. A comparison of the roof crush and ATD kinematics between the simulations with the original and a strengthened roof is shown in Figure 5. Apart from the extent of the roof crush, the main difference was that the FE ATD's head stayed in contact with the far-side roof rail in the case of a stronger roof, while it was pushed towards the near side by the crushing roof in the case of with the lower roof strength. This contrasted to the experimental test with the weak-roof vehicle, where the ATD's head was mainly held (entrapped [18]) in close proximity of the far-side header rail during the roof crush. Moreover, the ATD neck load for the weak roof SUV [22] was around 10 kN whereas the simulated FE ATD load for the strong roof vehicle shown in Figure 6 was around 7.5 kN. This compares to the ATD's neck load of around 3 kN for the strong roof vehicle [23] tested using the CFIR JRS.

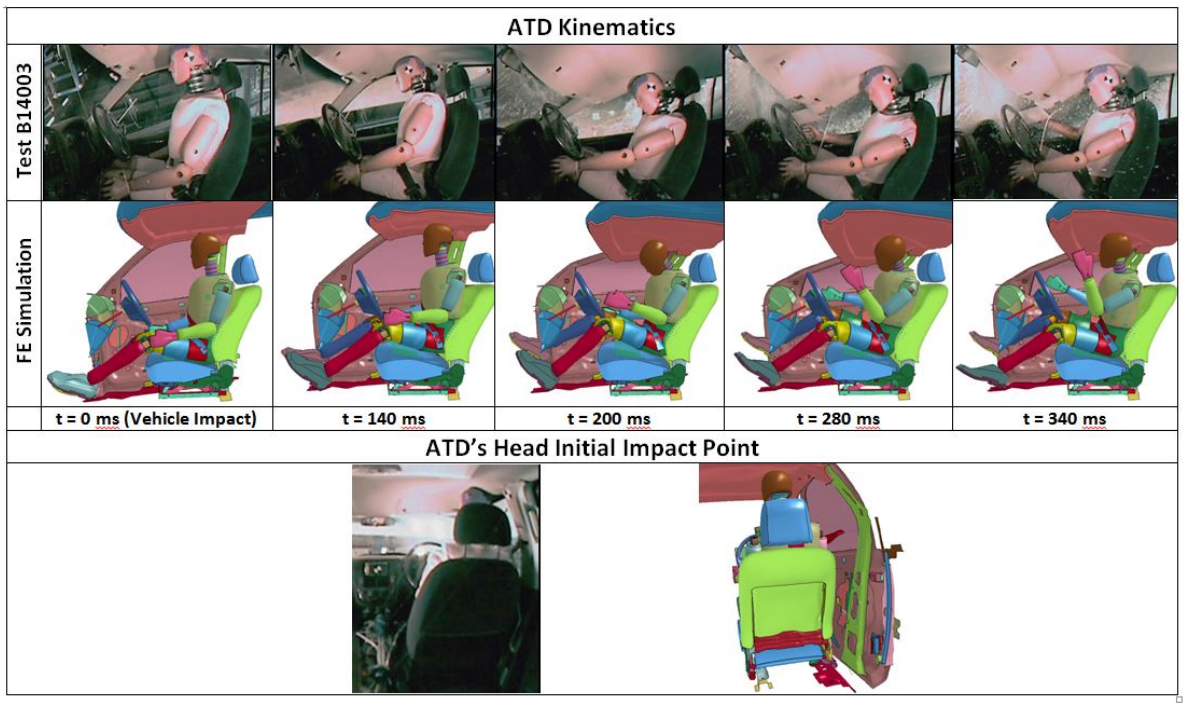

Figure 4. Experimental and simulated ATD kinematics and comparison of initial ATD head impact on vehicle roof [25,26,27].

The simulated angular speed of the FE ATD's head for both cases (original and strengthened vehicle roof) is shown in Figure 6. Although crush of the weak roof contributed to slowing the FE vehicle's roll motion as a result of dissipating more roll energy than in the case with a stronger roof, it caused the FE ATD's head to be pushed inboard (left bottom frame in Figure 5). This in turn resulted in a smaller upper-neck compressive peak load being imparted in the case with a weak roof compared to the case with a strengthened roof. In fact, in the case with a weak roof the FE ATD head was forced to tilt laterally with a consequent bending of the neck, which mitigated the compressive load applied onto the neck.

A possible explanation for the apparently opposite trends in terms of neck loading when comparing the CFIR JRS experimental test results and the FE simulations is related to the different magnitudes of roof crush that occurred in the weak-roof vehicle used in the experimental test compared with the FE vehicle model in the simulations. Also the interior shapes and sizes of the Jeep Grand Cherokee and Ford Explorer interior is different to the Volvo XC90 causing the head to interact and move differently within the vehicle when in contact with the roof, i.e. the head tilts rather than becoming entrapped.

In the experimental test, the weak-roof vehicle (i.e., Jeep Grand Cherokee) underwent larger roof crush than what was observed in the FE simulation using the original Ford Explorer FE model. A bimodal non-linear relationship between neck axial loading and the amount of roof crush seems to be consistent with a recent analysis of real-world NASS CDS rollover crashes conducted by Bambach et *al.* [5] as shown in Figure 7. In that study, a higher frequency of AIS 3+ occupant neck and spine injuries was found for either relatively small or very large magnitudes of vertical roof crush. However, the number of AIS 3+ injuries was reduced for magnitudes of roof crush between these two extremes.

A similar relationship would be expected between the neck axial compressive load and increasing amount of roof crush (or weaker roof), assuming that neck axial compression was causal to the cervical and upper thoracic spine injuries. Indeed, this trend was observed when comparing the simulated FE ATD neck load obtained using the Ford Explorer FE model when the roof was further weakened as shown in Figure 7. The FE ATD's Neck load for the 'weaker roof' (green curve) increased in magnitude compared to the 'weak roof' (red dashed cure). In other words, a very weak roof will likely result in increased neck loading. As a further observation, bending of the neck during roof crush may also be affected by other factors, such as localised buckling of the roof structure and/or roof interior padding. These factors, may contribute to either entrapping the head in position [18] or force it to move laterally. Whilst more detailed simulation work needs to be carried out, it appears that the orientation of the head relative to the torso and head entrapment are critical factors in terms of axial compressive loads imparted to the occupant's head during a rollover crash.

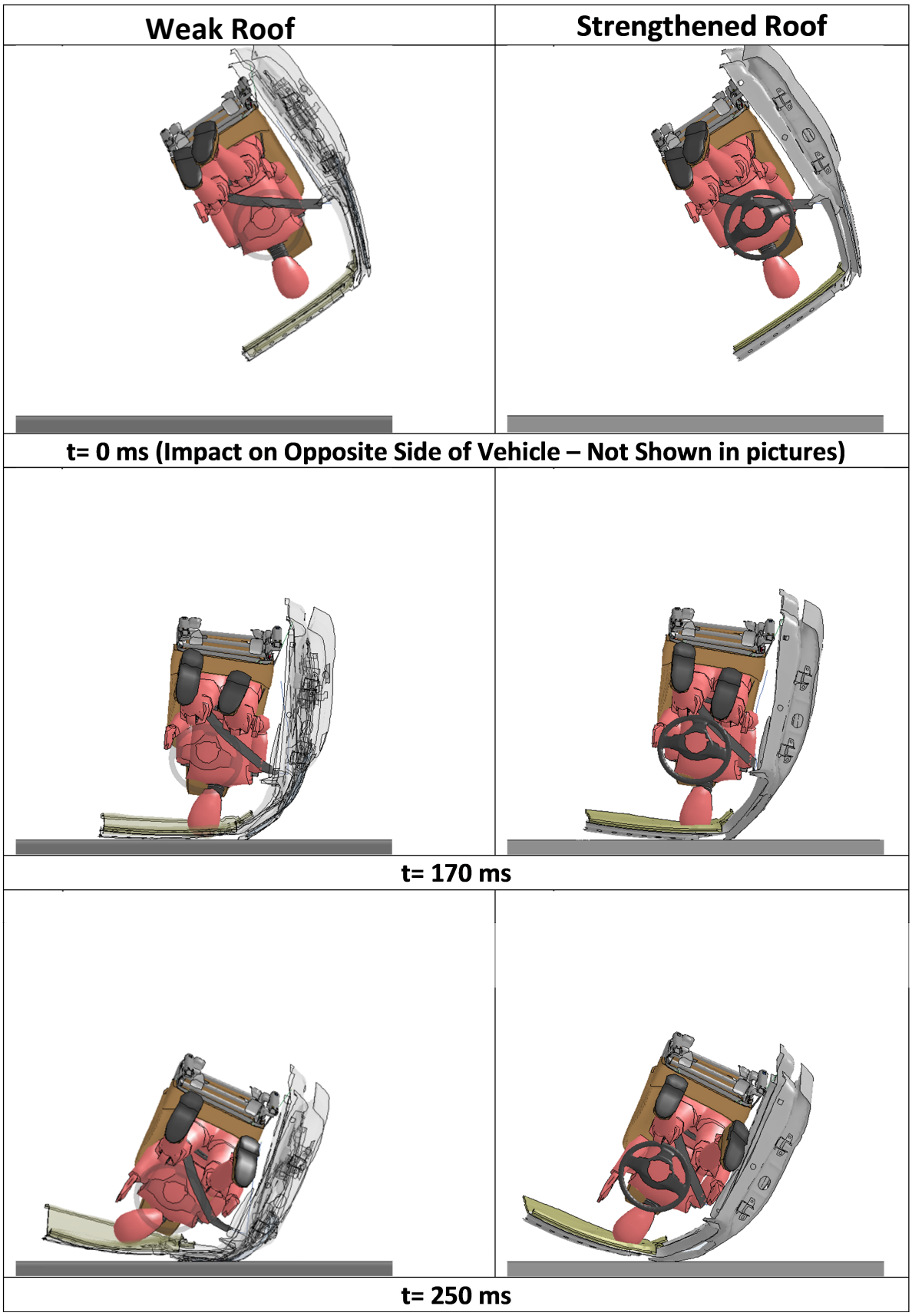

Figure 5. Simulated roof crush and FE ATD kinematics using Explorer model: strong (right) and weak (left) roof configurations.

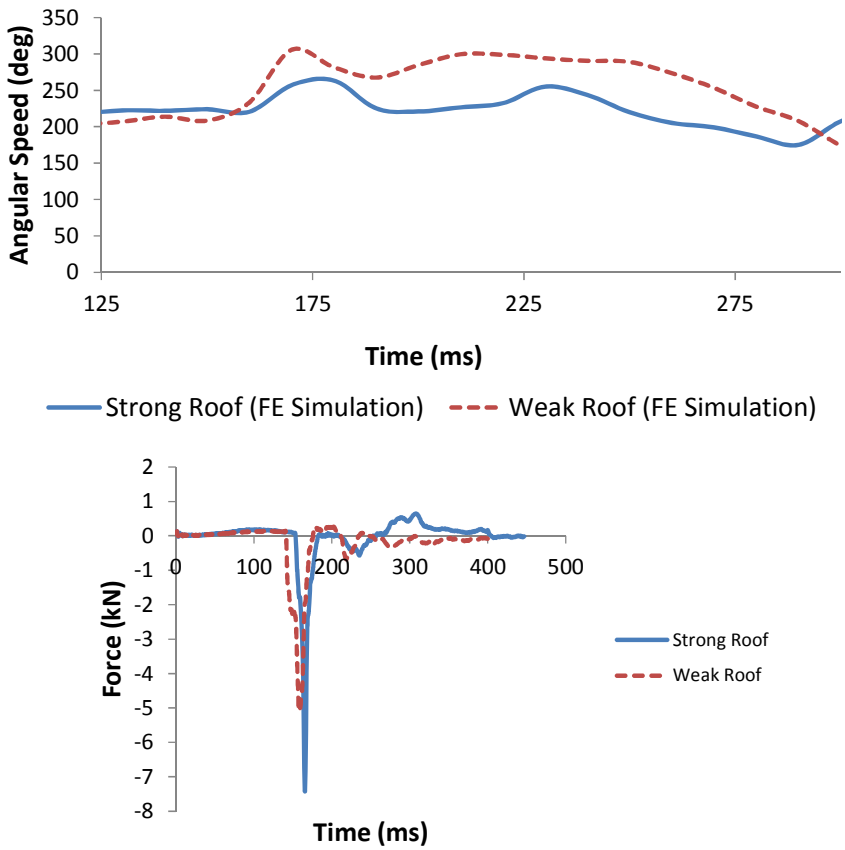

Figure 6. Simulated angular speed of the FE ATD head and upper-neck load: strong- and weak-roof configurations.

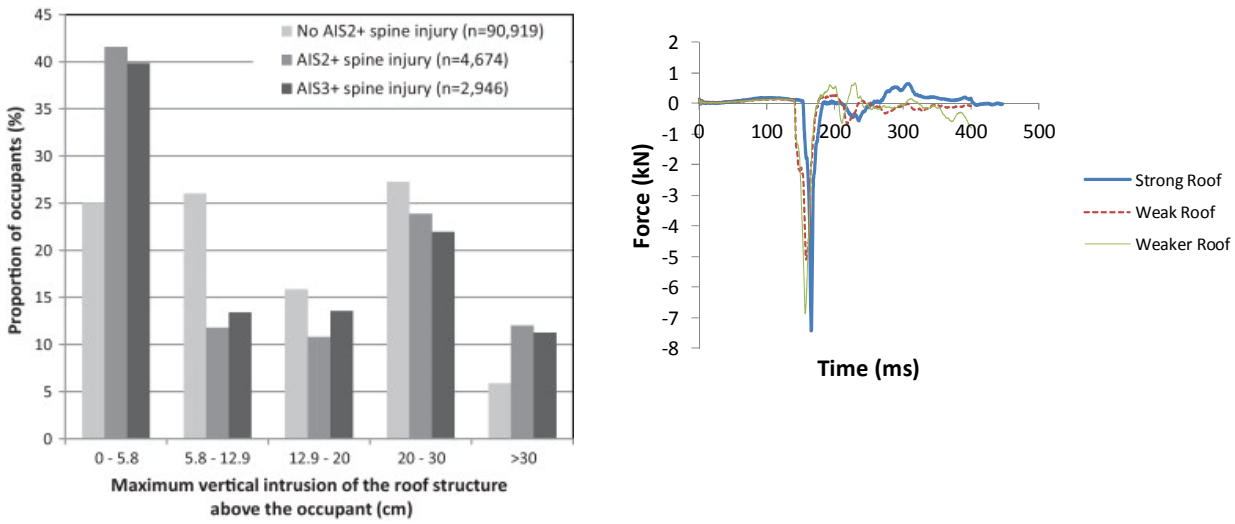

Figure 7. Distribution of occupant neck and spine injuries in rollover crashes based on vertical roof intrusion [5] (left) and simulated FE ATD neck load with a decreased levels of roof strength (right).

CONCLUSIONS

This paper describes how neck injuries can occur to a seat-belted occupant, seated in the front of the vehicle on the far-side opposite to the leading side of rollover, and are exacerbated in the case of a weak roof vehicle compared to a strong-roof vehicle. An analysis of experimental rollover crash test results, on two SUVs carried out using a JRS, indicate that in the case of a weak roof, the head can be entrapped within the crush zone. As a result, the distance between vehicle's CoG relative to the ATD's head increases to a lesser extent than in the case of a strong roof vehicle.

However, the analysis conducted using FE simulations resulted in different compressive neck loading with the FE ATDs. In the case of a weak roof, the simulated FE ATD's head was pushed towards the FE vehicle's near side exerted by the crushing far-side of the weaker roof. This had the effect of reducing the compressive peak load in the

FE ATD's neck. In contrast, in the strong roof FE Vehicle the FE ATD's head remained aligned with the torso and hence was subjected to a higher torso augmentation load (7.5 kN), albeit the load was less than that observed in the CFIR JRS tested weak roof vehicle (10 kN). This in turn indicates that inducing an offset to the head, e.g. side header rail air bag, that tilts the head inboard may alleviate the neck load in rollover crashes. This needs further investigation.

Whilst this analysis focused on the magnitude of the axial compressive force on the neck, which is indeed an important contributor to neck injury, future analysis should also consider neck flexion moments and shear forces. Although the Hybrid III is widely used for many crash applications, including rollover crash tests, the neck of the ATD has been observed to have limited biofidelity [30]. In particular, the neck response of the Hybrid III has been shown to be stiffer than the actual human neck [31]. Further investigations should be conducted using simulations with a detailed and validated human body FE model, such as the Total Human Model for Safety (THUMS) or Global Human Body Model Consortium (GHBMC). Ultimately, experimental tests with post-mortem human specimens should be considered as well.

ACKNOWLEDGEMENTS

The work described in this paper was part of the TARS UNSW Dynamic Rollover Protection (DROP) Project [27,32]. The authors would like to thank the Australian federal government's Australian Research Council for providing funds to carry out this research through the Linkage Projects grants scheme (No. LP110100069). The authors would also thank the industry partners for providing industry funding as Partner Organisation to the ARC Linkage project, namely, the New South Wales state government's Centre for Road Safety at Transport for New South Wales, the Victorian state government's third-party insurer Transport Accident Commission (TAC), the West Australian (WA) state government's Office of Road Safety at Main Roads WA, the mining company BHP Billiton Ltd., and the U.S. Center for Injury Research (CFIR).

The rollover crash test results [22,23] using the CFIR JRS was provided by the Center for Injury Research (CfIR). The authors would also like to acknowledge the staff at the Road and Maritime Services (RMS) Crashlab for the setup and carrying out of the rollover crash tests using the UNSW JRS and the Explorer vehicle for FE model calibration purposes [25,27].

REFERENCES

1 National Highway Traffic Safety Administration (NHTSA), Traffic Safety Facts 2012, A Compilation of Motor Vehicle Crash Data from the Fatality Analysis Reporting System and the General Estimates System, National Center for Statistics and Analysis, U.S. Department of Transportation, DOT HS 812 032, 2012.

2 Fréchède, B., McIntosh A.S., Grzebieta R.H., and Bambach M.R., (2010). "Characteristics of Single-Vehicle Rollover Fatalities in Three Australian States (2000-2007)." Accident Analysis and Prevention, Vol. 43, Issue 3, pp. 804-12.

3 Young, D., Grzebieta R.H., Rechnitzer G., Bambach M., and Richardson S., (2006). "Rollover Crash safety: Characteristics and Issues." 5th International Crashworthiness Conference (ICRASH 2006), Athens, Greece.

4 Grzebieta, R.H., Bambach M., McIntosh A.S., Digges K., Mattos G., Simons K., and Rechnitzer G., (2013). "Replicating Real-World Rollover Crash Injuries." 23rd International Technical Conference on the Enhanced Safety of Vehicles (ESV), Seoul, Korea.

5 Bambach, M., Grzebieta R.H., McIntosh A.S., and Mattos G., (2013). "Cervical and Thoracic Spine Injury from Interactions with Vehicle Roofs in Pure Rollover Crashes." Accident Analysis and Prevention, Vol. 50, pp. 34-43.

6 Moffatt E.A., (1975). "Occupant Motion in Rollover Collisions." 19th Conference of the American Association of Automotive Medicine. San Diego, California, USA.

7 Bahling, G. S., Bundorf R.T., Kaspzyk G.S., Moffatt E.A., Orlowski K.F., and Stocke J.E., (1990). Rollover and Drop Tests: The influence of Roof Strength on Injury Mechanics using Belted Dummies. SAE Paper 902314, Society of Automotive Engineers, Warrendale, PA, USA.

8 Piziali, R., Hopper R., Girvan D., and Merala R., (1998). Injury Causation in Rollover Accidents and the Biofidelity of Hybrid III Data in Rollover Tests. SAE Paper 980362, Society of Automotive Engineers, Warrendale, PA, USA.

9 James, M. B., Nordhagen R.P., Schneider D.C., and Koh S.W., (2007). "Occupant Injury in Rollover Crashes: A Reexamination of Malibu II." SAE Paper 2007-01-0369, Society of Automotive Engineers, Warrendale, PA, USA.

10 Grzebieta R.H., Young D., Bambach M., McIntosh A., (2007). Rollover Crashes: Diving Versus Roof Crush, Proc. 20th International Technical Conference on the Enhanced Safety of Vehicles, Lyon, France.

11 Brumbelow, M.L., Teoh E.R., Zuby D.S., and McCartt A.T., (2008). Roof Strength and Injury Risk in Rollover Crashes. Proceedings of the 2008 IRCOBI Conference, Bern, Switzerland.

12 Brumbelow, M. L. and Teoh E.R., (2009). Roof strength and injury risk in rollover crashes of passenger cars and SUVs. 21st International Technical Conference on the Enhanced of Safety of Vehicles (ESV), Stuttgart, Germany.

13 Friedman D. and Grzebieta.R.H., (2009). "A Proposed Rollover and Comprehensive Rating System." 21st International Technical Conference on the Enhanced Safety of Vehicles (ESV), Stuttgart, Germany.

14 Mandell S.P., Kaufman R., Mack C.D., and Bulger W.M., (2010). Mortality and Injury Patterns Associated with Roof Crush in Rollover Crashes. Accident Analysis and Prevention, Vol. 42, pp. 1326–1331.

15 Conroy, C., Hoyt D.B., Eastman A.B., Erwin S., Pacyna S., Holbrook T.L., Vaughan T., Sise M., Kennedy F., and Velky T., (2006). Rollover Crashes: Predicting Serious Injury Based on Occupant, Vehicle, and Crash Characteristics. Accident Analysis and Prevention, Vol. 38, pp.835-842.

16 Kahane, K.J. (1989). An Evaluation of Door Locks and Roof Crush Resistance of Passenger Cars – Federal Motor Vehicle Safety Standards 206 and 216, DOT HS 807 489, NHTSA Technical Report.

17 Strashny A. (2007). The Role of Vertical Roof Intrusion and Post-Crash Headroom in Predicting Roof Contact Injuries to the Head, Neck or Face During FMVSS No.216 Rollovers; An Updated Analysis. DOT HS 810 847.

18 Rechnitzer G. & Lane J., (1994) Rollover Crash Study - Vehicle design and occupant injuries. Monash University Accident Research Centre (MUARC) Report No. 65, Monash University, Melbourne, Australia.

19 Young, D.P., Grzebieta R.H., McIntosh A.S., Bambach M., and Fréchède B., (2007). Diving Versus Roof Intrusion: A Review of Rollover Injury Causation. International Journal of Crashworthiness, Vol. 12, Issue 6, pp. 609-628.

20 Grzebieta, R.H., McIntosh A.S., and Bambach M., (2010). How Stronger Roofs Prevent Diving Injuries In Rollover Crashes. In Proceeding of the 7th International Crashworthiness Conference (ICRASH), Washington D.C, USA.

21 Jordan, A. and Bish J., (2005). Repeatability Testing of a Dynamic Rollover Test Fixture. In Proceedings of the International Technical Conference on the Enhanced Safety of Vehicles (ESV), Paper Number 05-0362, Washington D.C., USA.

22 Center for Injury Research (CfIR), (2008). JRS Dynamic Rollover Test of a 2007 Jeep Grand Cherokee." Test Report submitted to Santos Family Foundation.

23 Center for Injury Research (CfIR), (2009). JRS Dynamic Rollover Test of a 2005 Volvo XC90. Test Report submitted to Santos Family Foundation.

24 Hallquist, J.O. (2014). LS-DYNA - Keyword User's Manual LS-DYNA R 7.1 (revision: 5471). Livermore Software Technology Corporation (LSTC), Livermore, CA.

25 Mongiardini, M., Mattos G., and Grzebieta R., (2014). Computer Modelling of a Test Device for Investigating Injury Causes in Vehicle Rollovers. Journal of the Australasian College of Road Safety, Vol. 25, No. 2, pp. 16-23.

26 Mongiardini, M., Grzebieta R., and Mattos G., (2015). Computer Modelling of Vehicle Rollover Crash Testing with the UNSW JRS. (In Preparation).

27 Grzebieta, R., McIntosh A., Mattos G., Simmons K., Rechnitzer G., Mongiardini M., Dal Nevo R., and Jackson C., (2013). Implementation of the UNSW Jordan Rollover System at Sydney's Crashlab Test Facility. In Proceeding of the International Technical Conference on the Enhanced Safety of Vehicles (ESV), Paper Number 13-0120, Seoul, Republic of Korea.

28 National Crash Analysis Center (NCAC), (2014). Finite Element Model Archive. http://www.ncac.gwu.edu/vml/models.html (Last accessed: Sep. 19, 2014).

29 Livermore Software Technology Corporation (LSTC), (2015). Dummy and Barrier Models for LS-DYNA:. http://lstc.com/download/dummy_and_barrier_models (Last accessed: Jan. 19, 2015).

30 Fréchède BO, McIntosh AS, Grzebieta RH & Bambach M, (2009) Hybrid III ATD in inverted impacts: influence of impact angle on neck injury risk assessment, Annals of Biomedical Engineering; 37: 1403-1414.

31 McIntosh A.S., Frechede B., Grzebieta R.H. and Bambach M.R., (2010). Biomechanical considerations for a dynamic rollover crash test, Proc. 7th Int. Crashworthiness Conf. ICRASH 2010, ed. Chirwa E.C. and S. Kan, Washington DC.

32 Grzebieta R.H., Bambach M., McIntosh A.S., Digges K., Mattos G., Simons K., Rechnitzer G., (2013). Replicating Real World Rollover Crash Injuries, Proc. 23rd International Technical Conference on the Enhanced Safety of Vehicles, Seoul, Korea, Paper Number 13-0098-O.